BIOCHEMISTRY
including biophysical chemistry & molecular biology

Article

pubs.acs.org/biochemistry

Deconstruction of Activity-Dependent Covalent Modification of Heme in Human Neutrophil Myeloperoxidase by Multistage Mass Spectrometry (MS^4)

Kieran F. Geoghegan,* Alison H. Varghese, Xidong Feng, Andrew J. Bessire, James J. Conboy, Roger B. Ruggeri, Kay Ahn, Samantha N. Spath, Sergey V. Filippov, Steven J. Conrad, Philip A. Carpino, Cristiano R. W. Guimarães, and Felix F. Vajdos

Pfizer Worldwide Research, Groton, Connecticut 06340, United States

Supporting Information

ABSTRACT: Myeloperoxidase (MPO) is known to be inactivated and covalently modified by treatment with hydrogen peroxide and agents similar to 3-(2-ethoxypropyl)-2-thioxo-2,3-dihydro-1*H*-purin-6(9*H*)-one (**1**), a 254.08 Da derivative of 2-thioxanthine. Peptide mapping by liquid chromatography and mass spectrometry detected modification by **1** in a labile peptide−heme−peptide fragment of the enzyme, accompanied by a mass increase of 252.08 Da. The loss of two hydrogen atoms was consistent with mechanism-based oxidative coupling. Multistage mass spectrometry (MS^4) of the modified fragment in an ion trap/Orbitrap spectrometer demonstrated that **1** was coupled directly to heme. Use of a 10 amu window delivered the full isotopic envelope of each precursor ion to collision-induced dissociation, preserving definitive isotopic profiles for iron-containing fragments through successive steps of multistage mass spectrometry. Iron isotope signatures and accurate mass measurements supported the structural assignments. Crystallographic analysis confirmed linkage between the methyl substituent of the heme pyrrole D ring and the sulfur atom of **1**. The final orientation of **1** perpendicular to the plane of the heme ring suggested a mechanism consisting of two consecutive one-electron oxidations of **1** by MPO. Multistage mass spectrometry using stage-specific collision energies permits stepwise deconstruction of modifications of heme enzymes containing covalent links between the heme group and the polypeptide chain.

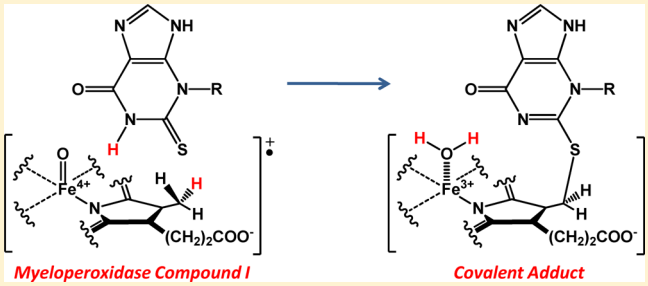

The heme prosthetic group gives biological systems access to redox chemistries that exceed the capacities of simple polypeptides, and heme peroxidases are among the many specialized types of enzyme that use it. They are not exclusively mammalian, but their vast and varied importance in human biology and health has created a focus on the several mammalian examples.[1−4] These include lactoperoxidase, an antimicrobial component of milk; thyroperoxidase, which catalyzes iodination and conjugation of tyrosine-derived intermediates to synthesize thyroid hormones; eosinophil peroxidase, deployed in the body's defense against parasites; and myeloperoxidase (MPO), a defensive chemical warfare agent against bacterial pathogens.

The signature activity of MPO is a two-electron oxidation of chloride to hypochlorous acid/hypochlorite.[5] Similar reactions are catalyzed with additional inorganic substrates, including thiocyanate[6] and other halides,[1] but MPO also converts organic substrates to reactive products that engage in tissue-damaging reactions. A recently proposed example is uric acid, elevated in gout to levels at which its oxidation by MPO may be significant.[7]

For all these reactions, MPO must itself first be oxidized from its ground state by hydrogen peroxide. H_2O_2 is provided by the action of NADH oxidase. It converts the resting enzyme [with Fe(III) of the heme group coordinated to water] to a reactive form called compound I, in which the transition to Fe(IV) accounts for departure of one electron from the enzyme and creation of an organic heme radical accounts for loss of a second. Substrates are then stripped of one or two electrons as completion of the catalytic cycle returns MPO to its resting state.

The destructive capability of MPO can injure host tissue as well as helping to destroy pathogens, and MPO is increasingly seen as an agent of self-injury that contributes to neuro-inflammation,[8] smoking-induced illness,[9] and cardiovascular disease.[10] For this reason, MPO is now a target of drug discovery.[11]

Inactivation of MPO by propylthiouracil[12,13] foreshadowed the recent discovery that thioxanthine-related agents are

Received: December 18, 2011
Revised: February 17, 2012
Published: February 21, 2012

dx.doi.org/10.1021/bi201872j | *Biochemistry* 2012, 51, 2065−2077

mechanism-based inhibitors of MPO that covalently modify the heme group to inactivate the enzyme.[14] This strategy turns the enzyme's catalytic function against itself and falls into the broader category of chemical events in which heme-containing enzymes undergo modification of the heme system; examples of this abound (see Discussion). Closely aligned with these reactions are processes forming a late part of the assembly of mature MPO, in which three cross-linking reactions occur between the heme group and the polypeptide.[15,16] No other enzyme is involved, and the generation of reactive intermediates in the active site of MPO itself leads to the formation of ester links between hydroxymethyl substituents of heme and the side chain carboxylates of Asp260 and Glu408 as well as a unique sulfonium bond between Met409 and a heme vinyl group. These bonds form autocatalytically and contribute importantly to the functional properties and stabilization of the enzyme.[16,21]

Dissecting peroxidases or other heme enzymes that have undergone this type of reaction requires a combination of protein biochemistry and mass spectrometry and will be an essential activity as drug discovery against MPO and related targets proceeds.[17] In this study, we used a sequence of chemical and enzymatic cleavage reactions to excise a peptide−heme−peptide fragment of MPO and then used multistage mass spectrometry (MS^4) to deduce the site at which the enzyme had undergone covalent modification by 3-(2-ethoxypropyl)-2-thioxo-2,3-dihydro-1*H*-purin-6(9*H*)-one (**1**), a 254.08 Da derivative of 2-thioxanthine. This result was established elsewhere for a related compound by complete excision of heme from MPO,[14] but the alternative approach demonstrated here has particular features of interest. It relies on sequential gas-phase deconstruction of the conjugate using accurate mass measurements and the unique isotopic signature of iron to define the site at which heme was modified by a reactive derivative of **1**.

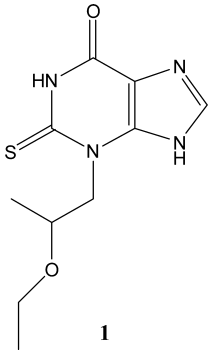

1

The work provides insight into the respective stabilities of the bonds holding major elements of this structure together and the specific dissociative pathways by which they break under collisional activation in the ion trap of a hybrid mass spectrometer (LTQ Orbitrap Velos, Thermo Scientific). The results and strategies described should assist further studies of MPO and other heme enzymes both before and after mechanism-based inactivation.

EXPERIMENTAL PROCEDURES

Enzyme. A solution of MPO isoform C isolated from human neutrophils was purchased (catalog no. 426-10C) from Lee Biosolutions Inc. (St. Louis, MO). The amino acid sequence numbering used in this paper refers to the canonical B form (UniProt entry P05164-1).

Reaction (example). Three milliliters of myeloperoxidase isoform C (MPO) was buffer-exchanged into 0.05 M sodium phosphate (pH 7.4) either by dialysis overnight at 4 °C against 1 L of the buffer (10K molecular weight cutoff Slide-A-Lyzer, Thermo Scientific) or using a 5 mL HiTrap Desalt column (GE Healthcare). The protein concentration was determined, and MPO was incubated at 24 °C for 30 min with a 100-fold molar excess of thioxanthine **1** (typically 1.2 mM) before being further treated with a 10-fold molar excess of H_2O_2 and incubated at 24 °C for 20 min. Control samples were treated with neither reagent nor H_2O_2 alone. The reaction mixture was next loaded at a rate of 1 mL/min onto a 1 mL HiTrap SP Sepharose column equilibrated with 50 mM sodium phosphate (pH 7.4), and the column was washed with 10 mL of the same buffer at a rate of 1 mL/min. MPO was then eluted with a gradient of NaCl in the same buffer (0.0 to 1.0 M NaCl at a rate of 1 mL/min over 10 min), with 2 mL fractions collected. Fractions containing MPO were pooled and concentrated as necessary for future uses, such as crystallization.

Digestion. Control, H_2O_2-treated, or thioxanthine **1**- and H_2O_2-treated MPO (0.03 mL, 2.6−3.2 mg/mL) was diluted with 9 volumes of 0.16 M sodium acetate (pH 3.8), and solutions were concentrated to 0.05 mL using a Microcon-10 (Millipore). The concentrated samples were incubated at 95 °C for 10 min, then allowed to cool, and treated with 0.175 mL of 0.1 M NH_4HCO_3. One microgram of sequencing-grade trypsin (Promega) was added, and the samples were incubated at 24 °C for 7 h. The resulting digests were then analyzed by liquid chromatography and mass spectrometry (LC−MS) or stored at −80 °C.

Liquid Chromatography and Mass Spectrometry (LC−MS). Initial LC−MS peptide mapping studies were performed using a Vydac C18 capillary column (type 218MS5.510) with a gradient of acetonitrile in 0.02% TFA at a flow rate of 5 μL/min and an LTQ mass spectrometer (Thermo Scientific). Chromatography was conducted on an Agilent 1100 system that included a G1376A binary capillary pump and a G1315B diode-array detector collecting data at 220, 280, and 400 nm as well as peak absorption spectra. Nano-LC−MS was performed using an Eksigent (Dublin, CA) NanoLC-Ultra 2D Plus system coupled to an LTQ Orbitrap Velos spectrometer (Thermo Scientific). The nano-LC system consisted of a NanoLC-Ultra AS-2 autosampler linked to dual-gradient pumps (designated 1 and 2) and a loading pump. Gradient pump 2 was used both for sample loading at a rate of 510 nL/min and for gradient elution at a rate of 300 nL/min. The column was produced in house using a New Objective self-pack PicoFrit column (15 μm tip inside diameter) cut down to 30 cm and packed with Reprosil-Pur Basic-C18 3 μm resin (Dr Maisch GmbH) under a pressure of 2200 psi for 2 h. The C18 material was compacted further into ∼18 cm after an online LC−MS run with 0.1% formic acid as solvent A and 0.1% formic acid in acetonitrile as solvent B. A two-phase linear gradient from 5 to 50% B over 60 min and from 50 to 70% B over 15 min was employed. A specially made T-piece connector was used to connect the column directly with gradient pump 2 and provide electrical contact for the nanoelectrospray voltage (∼2.2 kV) through the liquid at the T-piece joint. The eluant was sprayed directly with slightly off-axis positioning to the inlet orifice of the mass spectrometer. The ions were sampled by the S-lens and transferred through a set of ion manipulation devices to the dual-pressure LTQ ion

dx.doi.org/10.1021/bi201872j | *Biochemistry* 2012, 51, 2065−2077

trap for precursor ion isolation and fragmentation or to the Orbitrap analyzer for full scan MS with a mass range of m/z 300−2000. A mass resolving power R of 30000 (fwhm) at m/z 400 was set for all Orbitrap analyzer measurements. The hybrid mass spectrometer was operated in the data-dependent mode such that once the predefined precursor ions were detected in the Orbitrap, they were isolated and fragmented in the high-pressure cell of the ion trap by CID with subsequent high mass accuracy and ultra-high-resolution detection in the Orbitrap analyzer. The normalized collision energy was set at 35% with an activation time of 10 ms for the majority of MS^n CID experiments. The fragment ions were detected with nearly complete attenuation of the precursor ion signal, except in the cases of MS^3 of the ion at m/z 1062.3 and MS^4 of the ion at m/z 1060.3, where the collision energy was lowered to 25% to detect fragment ions. Presumably, the precursor ions at m/z 1062.3 and 1060.3, generated from prior CIDs, were away from the ion trap center and could have been ejected out of the trap with a 35% activation energy. The LTQ Orbitrap Velos mass spectrometer was calibrated using a Thermo positive ion mode calibration solution (Calmix), and mass spectra were further calibrated off-line with RecalOffline (Thermo Scientific), using the identified MPO tryptic peptide (residues 198−218, WLPAEYEDGFSLPYGWTPGVK) at m/z 804.7231^{3+} and 1206.5810^{2+} detected in the same LC−MS ion chromatogram.

Isotope-specific masses reported herein are for the most abundant form, and electron masses are deducted from calculated mass values according to detected charge states. Mass errors (Δ) are expressed in parts per million {Δ(ppm) = [(experimental mass − predicted mass) × 10^6]/predicted mass}. To match the experimentally achieved resolutions, the mass resolving power (fwhm) set for isotopic simulations was 30000 for the m/z 658 or 656 ion clusters and 20000 for all other fragment ions.

Software. Calculations of theoretical molecular masses and spectral simulations were performed using GPMAW (Lighthouse software, Odense, Denmark), the ChemBioDraw Ultra version 11.0.1 module of ChemBioOffice 2008 (Cambridgesoft), and the QualBrowser version 2.0.7 module of Xcalibur (Thermo Scientific). Sequence database searches were conducted using Mascot (licensed from Matrix Science, Boston, MA).

Crystallization. Following cation-exchange chromatography, thioxanthine **1**- and peroxide-treated MPO was buffer-exchanged into 0.05 M sodium acetate, 0.05 M $(NH_4)_2SO_4$, and 2 mM $CaCl_2$ (pH 5.5) and then concentrated to 20 mg/mL. Sitting drops were set in a 96-well plate using a Mosquito liquid handler (TTP Labtech, Melbourn, Herts, U.K.). For each well, 300 nL of protein solution was mixed with an equal volume of well solution containing 27% PEG 3350 and 0.25 M $CaCl_2$ complemented with a corresponding Hampton Additive Screen HT condition (Hampton Research, Aliso Viejo, CA) at 22 °C. After 7 days, multiple hits were observed with a betaine hydrochloride additive, and these led to structural analysis.

Crystallography. A single crystal of **1**-modified MPO was transferred to a cryoprotectant solution consisting of 21.6% PEG 3350, 0.2 M $CaCl_2$, and 20% glycerol and immediately flash-cooled by immersion in liquid nitrogen. X-ray diffraction data were collected on a Pilatus 6 M pixel array detector (Dectris Ltd., Baden, Switzerland) at IMCA beamline 17ID at the Advanced Photon Source (Argonne, IL). A 180° sweep was collected in 0.25°, 0.25 s increments. Data were processed with AUTOPROC[18] (Global Phasing, Cambridge, U.K.), using XDS as the integration program[19] and programs from the CCP4 suite of crystallographic software.[20]

Computational Chemistry. Calculations of tautomeric equilibria were performed using the Jaguar software package (Schrödinger). B3LYP/6-311G** with solvent effects (water) included through the application of the Poisson−Boltzmann solver was used to calculate the difference in energy between the tautomeric forms.

RESULTS

Mass Spectrometry. The sulfonium bond between heme and the sulfur of Met409 was first defined by showing that both it and the Met409−Pro410 peptide bond were cleaved when MPO was treated with 0.16 M sodium acetate (pH 3.8) at 95 °C for 10 min [the original authors termed this reagent 1% acetic acid (pH 3.8)].[22,23] Applying this treatment to MPO, regardless of thioxanthine **1** treatment, was expected to create a new N-terminus at Pro410 and leave a methyl thioether substituent on the heme pyrrole A ring vinyl group.[22]

We used this reaction as the first step in digesting MPO for analysis of chemical changes at the heme group. The success of the reaction was indicated by the presence of a strong peak for the semitryptic fragment of residues 410−421 in tryptic LC−MS peptide mapping of the heat-treated protein (Figure 1).

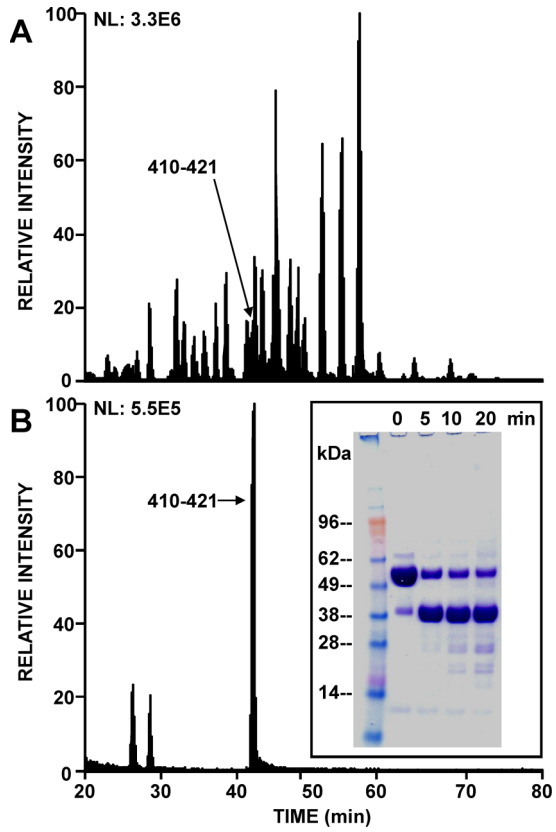

Figure 1. (A) LC−MS peptide mapping of MPO with an arrow indicating the peak of peptide 410−421. Cleavage of the Met409−Pro410 bond by heat treatment is required for the formation of this semitryptic peptide. The maximal intensity in instrument units (3.3E6) (NL, normalized level) is indicated beside the vertical axis. (B) Extracted ion plot for peptide 410−421 with a peak intensity of 5.5E5 or 17% of the base peak value. The inset shows Coomassie Blue-stained sodium dodecyl sulfate−polyacrylamide gel electrophoresis showing cleavage of MPO by incubation at pH 3.8 and 95 °C.

dx.doi.org/10.1021/bi201872j | Biochemistry 2012, 51, 2065−2077

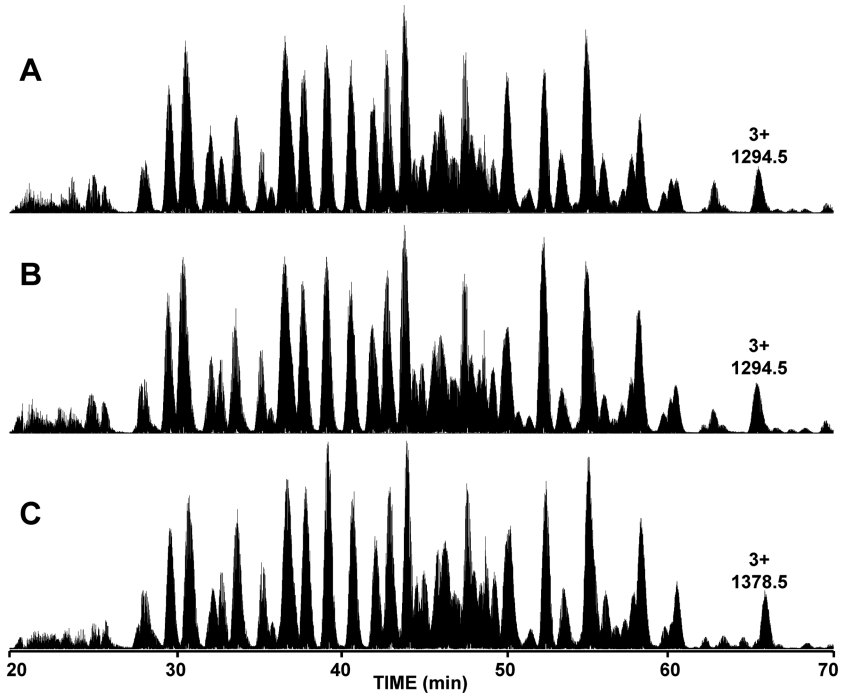

Figure 2. LC−MS peptide maps for (A) the MPO control sample, (B) MPO treated with H_2O_2, and (C) MPO treated with H_2O_2 and thioxanthine **1**. The m/z value (average mass) is shown for triply charged heme-containing peaks.

Reducing sodium dodecyl sulfate−polyacrylamide gel electrophoresis of treated MPO (Figure 1, inset) showed that a high fraction of the MPO heavy chain was cleaved to produce a new 38 kDa fragment. This mass was consistent with the predicted 410−745 fragment. The heat-driven cleavage was initially rapid, with a half-time of <5 min, but it did not go to completion. The reasons for this were not determined, but the result was the same for the control protein and for MPO treated with H_2O_2 in the presence or absence of thioxanthine **1**.

Protein treated with heat at pH 3.8 for 10 min was then used for further analysis. After addition of an ammonium bicarbonate solution, digestion was performed with trypsin. Disulfide bonds were not reduced. LC−MS peptide mapping of the digest was first performed by capillary high-performance liquid chromatography (Vydac C18) using an acetonitrile gradient in 0.02% TFA, and with ultraviolet−visible absorbance monitored prior to on-line mass spectrometry on an LTQ mass spectrometer.

The major 400 nm peak in a tryptic digest of heat-treated MPO was taken to be the principal heme-containing product (Figure S1 of the Supporting Information). Its corresponding mass peak contained a triply charged species with an m/z value close to 1294.5, as detected in full scan mode by an LTQ ion trap spectrometer (Figure 2A). This peak was also present in MPO treated with H_2O_2 only (Figure 2B). When MPO treated with H_2O_2 and the 254 Da thioxanthine **1** was subjected to the same analysis, the 3+ peak at 1294.5 was replaced by a 3+ peak at m/z ∼1378.5, a mass increase of 252 Da (Figure 2C). Maps for untreated and treated MPO were generally similar except for the change in the major heme-containing peak. Minor differences were attributed to products of incomplete digestion, because short digestion times (6 h at 24 °C with MPO at 0.5 μg/μL and trypsin at 0.005 μg/μL) gave better recoveries of the heme-containing peaks than longer digests. Detailed investigation of these products required a spectrometer with a higher mass resolution and a higher accuracy.

The LTQ Orbitrap Velos combines an Orbitrap mass analyzer with novel devices that include a dual-pressure ion trap.[24] This work required joint application of the ion trap's capacity for MS^n experiments and the FTMS-based highly accurate and highly resolving detection afforded by the Orbitrap analyzer.

Figure 3A shows the full FTMS spectrum of the major heme species from MPO not treated with **1**. If full and specific tryptic cleavage was allowed, heme was predicted to be ester-linked through Asp260 to the tryptic 249−272 fragment and through Glu408 to the Ser-Ser-Glu-Hsl peptide, where Hsl is homoserine lactone resulting from the bond-breaking heat step.[22] With heme taken as the cationic Fe^{3+} form, the 3+ species was envisioned as $[M + 2H]^{3+}$, and an elemental composition of $C_{177}H_{244}N_{40}O_{50}S_3Fe^{3+}$ was proposed for the doubly protonated triply charged product of electrospray ionization (Scheme 1.; the structures shown in the schemes do not include protonation). The simulated mass spectrum for this species agreed closely (Δ = −1.5 ppm) with the experimental spectrum collected in the Orbitrap (Figure 4A), including the presence of two minor peaks introduced by the 5.8% fractional abundance of the ^{54}Fe isotope and corresponding to the ^{54}Fe monoisotopic and $^{54}Fe^{13}C$ isotopic forms, respectively (see below).

In view of the 4 m/z unit width of the isotopic profile (Figure 4A) and an intent to pass the full isotopic set into CID, the isolation width parameter for all CID experiments was set to 10 m/z units. This determined that the precursor species for CID included ions at m/z values from 5 units below to 5 units above the nominal parent m/z value. MS^2 nominally performed on the m/z 1294.5 precursor should therefore apply CID to all ions ranging from m/z 1289.5 to 1299.5, allowing the isotopic profile of daughter ions to be observed. Fragments containing Fe^{3+}-heme should exhibit the characteristic isotopic profile due to the iron isotopes. Experimental data showed that this was

dx.doi.org/10.1021/bi201872j | *Biochemistry* 2012, 51, 2065−2077

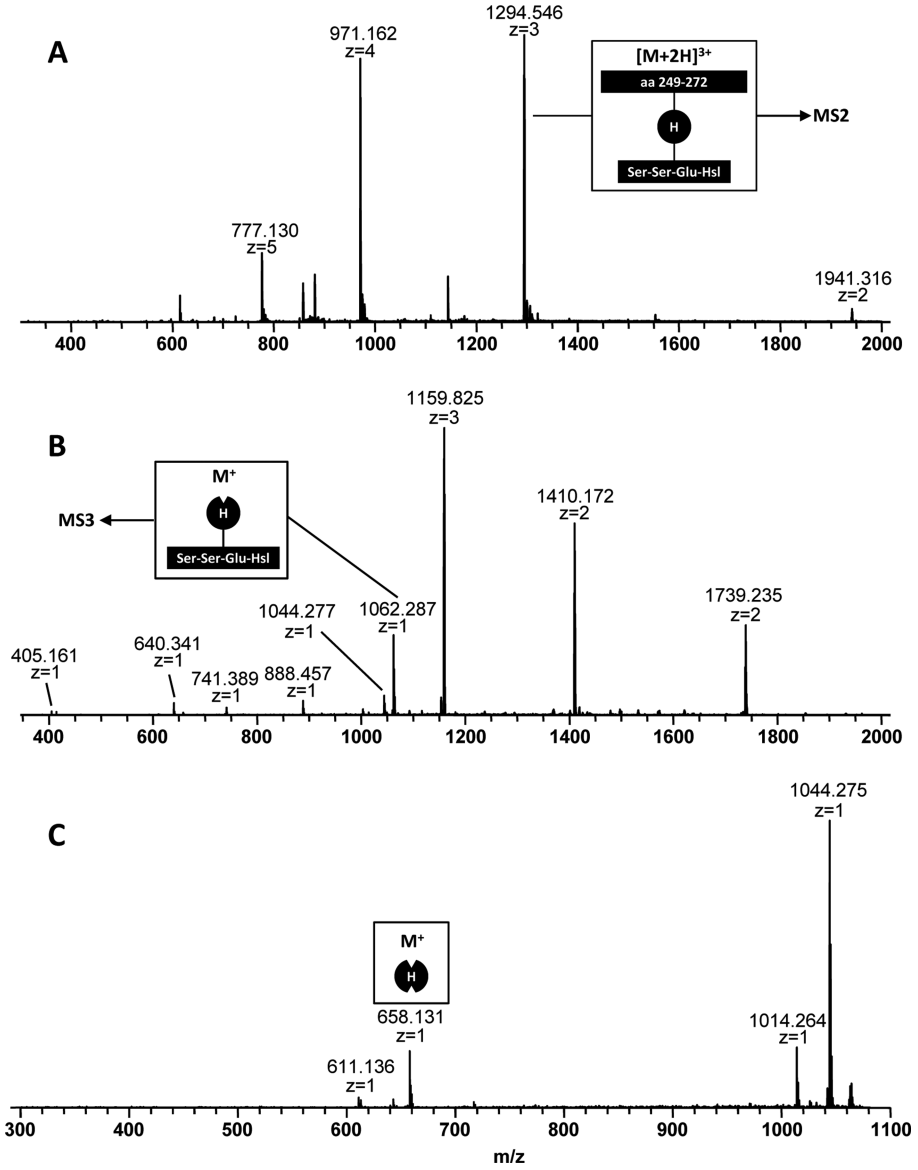

Figure 3. LC–MS peptide mapping of MPO with no thioxanthine **1** treatment. (A) Full mass spectrum with peaks corresponding to heme–peptide–heme fragment of MPO. Peak charge states are indicated by values of *z*, and the inset cartoon shows the structure assigned to the peak at *m*/*z* 1294.546, the parent ion for MS^2. (B) MS^2 spectrum for the peak at *m*/*z* 1294.546. The cartoon shows a notch in the heme group representing loss of 2 Da caused by dissociation of peptide 249–272 and the structure of the *m*/*z* 1062.287 peak selected for MS^3. (C) MS^3 spectrum in which the peak at *m*/*z* 658.131 is identified as the heme group having lost both peptide moieties.

achieved and facilitated the elucidation of structural information.

CID of the ion at *m*/*z* 1294.546 afforded a spectrum with four main features and significant additional peaks (Figure 3B). The major events were largely alternative dissociative events at the ester bonds linking heme to the two peptides. This was consistent with the selective nature of CID in the ion trap, where radiofrequency field oscillation is targeted specifically to a selected precursor ion and daughter ions do not receive activation.

The ions at *m*/*z* 1159.825 (Δ = −1.29 ppm) and *m*/*z* 1739.235 (Δ = −0.46 ppm) were $[M + 2H]^{3+}$ and $[M + H]^{2+}$, respectively, for heme linked to peptide 249–272 but with loss of the 406–409 peptide lactone (404.154 Da in free peptide form). In the triply charged parent, one charge is associated with heme, and the two protonations can be either split between the two peptide moieties or both located on peptide 249–272. In the first case (one proton on each peptide), dissociation of peptide 406–409 gives the small peak for $[M + H]^+$ of this peptide at *m*/*z* 405.161 (Δ = −0.99 ppm), and $[M + H]^{2+}$ at *m*/*z* 1739.235 for heme linked to peptide 249–272. In the second case (both protons on peptide 249–272), residues 406–409 depart as a neutral loss of 404.154 Da, leaving $[M + 2H]^{3+}$ at *m*/*z* 1159.825 for heme linked to residues 249–272.

When the other ester bond was broken, the singly charged peak at *m*/*z* 1062.287 (Δ = −0.47 ppm) was M^+ for heme remaining conjugated to peptide 406–409 lactone after dissociation of peptide 249–272 (Figure 4B for the peak and simulation and Scheme 1. for the structure). The same event generated the ion at *m*/*z* 1410.172 (Δ = 0.28 ppm) for $[M + 2H]^{2+}$ for peptide 249–272.

Peptides were eliminated by a pathway that was locally one of neutral loss, although the dissociating species could carry

dx.doi.org/10.1021/bi201872j | *Biochemistry* 2012, 51, 2065–2077

Scheme 1. Sequential Collision-Induced Dissociations of Unmodified Peptide-Heme-Peptide Fragment of MPO. Text in boxes represents 1-letter amino acid code.

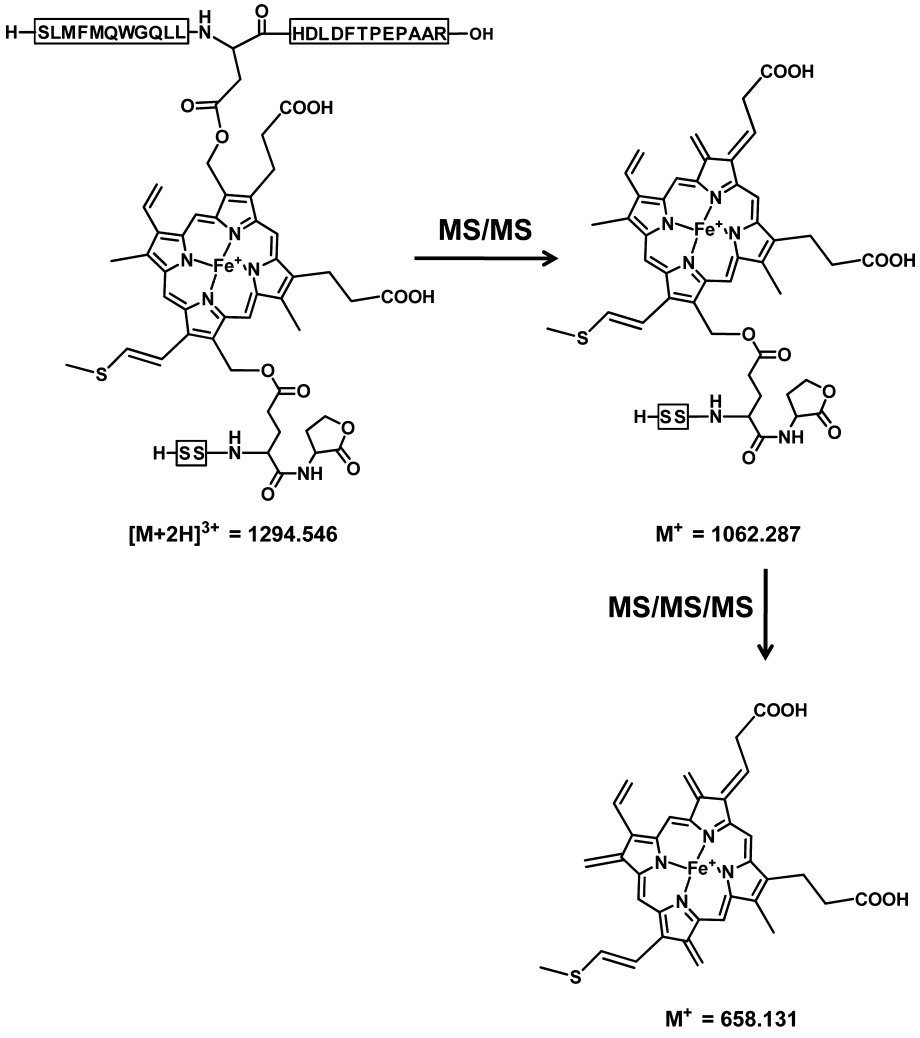

charge elsewhere. However, the side chain of Asp260 or Glu408 departed as the charge-neutral free acid (-COOH). This always left the corresponding heme product with an extra unsaturation, newly lacking 2 Da relative to its structure before it was hydroxylated prior to esterification with the peptide.

Less abundant fragment ions resulting from amide bond cleavages along the backbone of tryptic peptide 249−272 were also detected. Among them was the continuous series of y_4^+–y_{11}^+ ions as well as y_{12}^{2+}, none of which includes the heme attachment site at Asp260. Heme-containing fragment ions (with the 406−409 peptide eliminated from heme), b_{14}^{2+}, b_{17}^{2+}, b_{18}^{2+}, b_{20}^{2+}, and y_{19}^{2+}–y_{21}^{2+}, were also detected, consistent with the previous assignment for the heme attachment site.

MS^3 of the peak at m/z 1062.287 gave a daughter peak at m/z 658.131 (Figures 3C and 4C; $\Delta = -3.04$ ppm), which was in good agreement with the M^+ for the heme group including the two extra unsaturations caused by dissociation of the two peptides (Scheme 1.). The presence of an iron atom was clear from its characteristic isotopic distribution (Figure 4C) and the specific mass spacing between ^{54}Fe and ^{56}Fe (experimental, 1.996 Da; predicted, 1.995 Da). The use of accurately measured mass intervals between isotopes is an increasingly valued tool in structural assignments.[25,26]

Next, a similar study of the new peak created in the peptide map (Figure 2C) when MPO was treated with H_2O_2 and thioxanthine **1** ($C_{10}H_{14}N_4O_2S$, 254.0837 Da) was undertaken. Earlier work made it plausible that MPO was inactivated by covalent modification with **1**, possibly at the heme group or possibly by reaction at an amino acid side chain; as noted, this ambiguity was recently resolved by another route.[14] The 3+ peak at m/z 1378.5 in the moderate-resolution LTQ instrument represented a mass shift from the $[M + 2H]^{3+}$ fragment at m/z 1294.5 from unmodified MPO of 3×84.0 Da = 252.0 Da. As the mass of **1** is 254 Da, the result suggested addition of **1** to MPO with loss of H_2, which was consistent with the oxidative action of MPO and the earlier conclusion that this was a mechanism-based inactivation. The structure inset in Figure 5A was proposed as a working model, but it remained to be determined whether **1** had reacted at the heme group or on one of its ester-linked peptide substituents. A simulated mass spectrum for $[M + 2H]^{3+}$ of the proposed adduct with an elemental composition of $C_{187}H_{256}N_{44}O_{52}S_4Fe^{3+}$ agreed well with the Orbitrap spectrum of m/z 1378.572 (Figure S2A of the Supporting Information).

During MS^2 of the triply charged ion at m/z 1378.572 (Figure 5B), the major peak was triply charged with an ion at m/z 1293.872, a loss of m/z 84.70 from the triply charged

dx.doi.org/10.1021/bi201872j | *Biochemistry* 2012, 51, 2065−2077

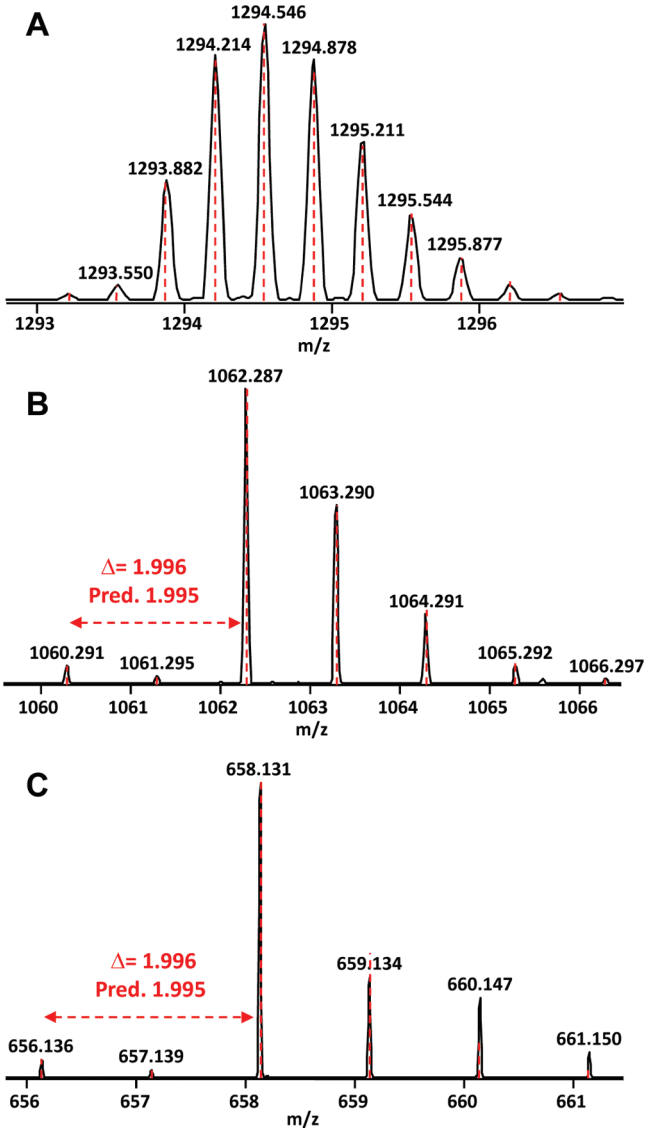

Figure 4. Experimental (curve, black line) and simulated (sticks, red dashed line) mass peaks for three important ions in Figure 3.

parent, and consistent (predicted, 1293.8724; Δ = −0.08 ppm) with loss of 254.10 Da (3 × 84.70 Da) from the parent. This suggested that **1**, which had been added with the loss of H_2, dissociated from the parent in its neutral 254 Da original form. Critically, this dissociation should leave a mass deficit of 2 Da relative to the unmodified MPO fragment at the site of thioxanthine **1** attachment. The isotopic cluster around *m/z* 1293.9 was correctly simulated by assuming loss from the parent species of the 254 Da thioxanthine **1** (Figure S2B of the Supporting Information).

The results of two further experiments ultimately indicated that **1** had been coupled to the heme group.

First, MS^3 of the *m/z* 1293.8^{3+} daughter of *m/z* 1378.5^{3+} (Figure 5C) gave peaks that excluded both peptide components from being the coupling point for **1**. Peptide 249–272 was detected as the same $[M + 2H]^{2+}$ product at *m/z* 1410.173 (Δ = 1.13 ppm) as had been dissociated from the unmodified peptide–heme–peptide fragment (Figure 3B). Peptide 406–409 lactone dissociated as $[M + H]^+$ = 405.162 (Δ = 0.0 ppm). By a process of exclusion, this indicated that the heme group must be the attachment point for **1**, because neither peptide had undergone the loss of 2 Da that accompanied dissociation of **1**.

Second, and more directly, MS^4 of the *m/z* 1060.3 peak gave a principal product ion at *m/z* 656.116 (Figure 5D), interpreted as M^+ for the heme group with a 2.015 Da mass deficiency compared to the form detected by MS^3 from the unmodified peptide–heme–peptide fragment (*m/z* 658.131 in Figure 3C). This result was consistent with the *m/z* 658.131 and 656.116 species differing in composition by two hydrogen atoms (theoretical mass discrepancy of 2.016 Da for two H atoms). Close inspection of the isotopic peak cluster around *m/z* 656.1 confirmed the presence of the iron signature, and simulation based on the elemental composition of the proposed M^+ gave a spectrum that agreed with experiment (Figure S2D of the Supporting Information).

Scheme 2 presents structures for the parent peptide–heme(**1**)–peptide fragment of MPO and the proposed CID intermediates.

X-ray Crystallography. Following crystallization of **1**-modified MPO and collection of beamline data, the structure was determined by molecular replacement using the CCP4 program *Phaser*.[27] Data statistics are reported in Table 1A. The Matthews volume of the unit cell indicated a high likelihood of four dimers of MPO per asymmetric unit. Using the structure of the MPO dimer, PDB entry 1CXP,[28] all four dimers were positioned in the asymmetric unit. Following initial rounds of refinement using REFMAC,[29] visual inspection of the electron density maps indicated strong $F_o - F_c$ density (>7σ) sprouting from the heme pyrrole D-ring methyl substituent. Lower-level contouring of $2F_o - F_c$ maps allowed for positioning of **1** consistent with a covalent (1.7 Å) bond between the S atom of **1** and the D-ring methyl carbon. Of the eight crystallographically distinct MPO monomers in the crystal, compound density was excellent for three (monomers A, E, and I), reasonable for two (J and M), and weak for three (B, F, and N). Despite the varying levels of order and/or occupancy at the different heme sites, the $F_o - F_c$ density immediately adjacent to the D-ring methyl indicated covalent modification at all eight active sites. Typical $(NAG)_2$-$mannose_3$ glycosylation was observed to varying degrees at Asn355, Asn391, and Asn483. Refinement statistics are listed in Table 1B.

The structure of MPO belongs to the heme-dependent peroxidase superfamily, consisting of 26 α-helices arranged around the central heme moiety.[30] The C-terminus of the MPO light chain sits at the entrance to the active site cavity. Thioxanthine **1** sits nearly orthogonal to the plane of the heme (Figure 6A), with the thioxanthine ketone oxygen participating in a hydrogen bond to the water molecule at the location recognized as the peroxide/halide binding site.[28,31] This water in turn is hydrogen-bonded to the Fe-coordinated water that presumably serves as the source of the oxygen atom during the formation of the oxo–Fe intermediate, compound I. The thioxanthine effectively fills the entrance to the active site cavity and may exert its inhibitory effect by blocking access of substrates to the heme (Figure 6B). The ethyl-isopropyl ether side chain emanating from the thioxanthine N3 atom is relatively poorly ordered in all eight molecules but appears to project out along the floor of the active site entrance.

■ DISCUSSION

Activity-dependent irreversible inactivation of MPO by **1** is presumably due to an underlying covalent event. Known mechanisms include cross-linking of **1** to an amino acid side

dx.doi.org/10.1021/bi201872j | *Biochemistry* 2012, 51, 2065–2077

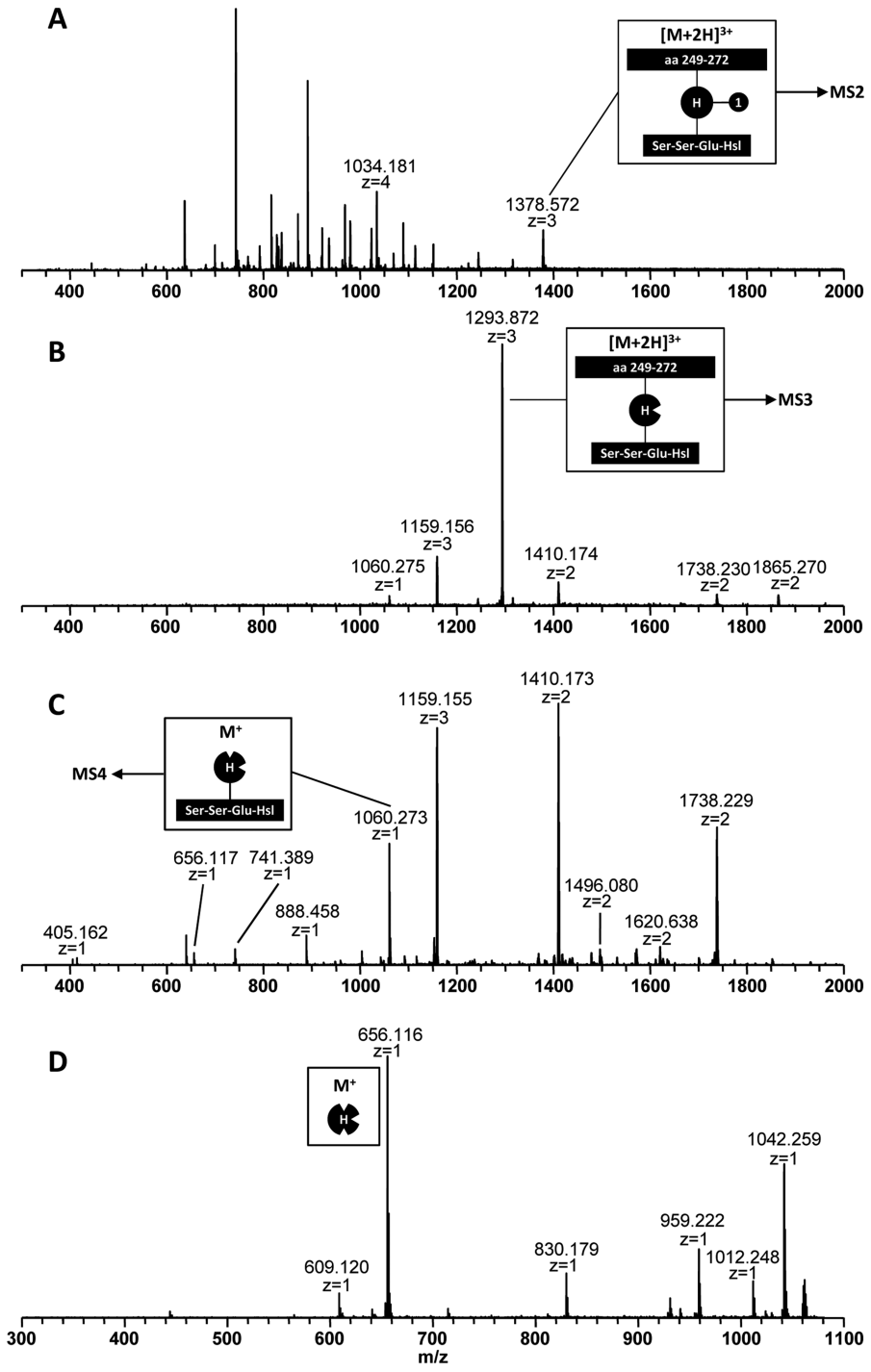

Figure 5. (A) Full mass spectrum of the peak containing the heme−peptide−heme fragment of MPO modified by thioxanthine **1**. The triply charged peak at m/z 1378.572 was identified as the species of interest and selected as the parent ion for MS^2. (B) MS^2 for the peak at m/z 1378.572. Here, the notch in the heme group represents the mass deficiency created by dissociation of the 254 Da thioxanthine **1** moiety, addition of which to heme added 252 Da. (C) MS^3 of the peak at m/z 1293.872. (D) MS^4 of the daughter ion at m/z 1060.273 from MS^3. The heme peak at m/z 656.116 was 2.015 Da lighter than the corresponding peak seen in Figure 2C.

chain or heme[32] and cross-linking of an amino acid side chain to heme,[33] any of which might occur by a mechanism requiring induction of a protein free radical.[34] Covalent attachments of inactivating agents to heme have previously been proposed, mainly on the basis of absorption spectroscopy, for several cases involving mammalian peroxidases,[32,35,36] but reviews have noted that the site and exact manner of conjugation are usually unknown.[11] Improved methods and strategies for clarifying these outcomes are required.

The mammalian/animal peroxidases are unusual in that their heme prosthetic groups are covalently linked to their polypeptides.[37] In this work, peptide mapping of control and inactivated MPO placed the site of modification in a peptide−heme−peptide product obtained by site-specific thermal cleavage[22] followed by tryptic digestion. Multistage mass

dx.doi.org/10.1021/bi201872j | *Biochemistry* 2012, 51, 2065−2077

Scheme 2. Sequential Collision-Induced Dissociations of Thioxanthine 1-Modified Peptide-Heme-Peptide Fragment of MPO. Text in boxes represents 1-letter amino acid code.

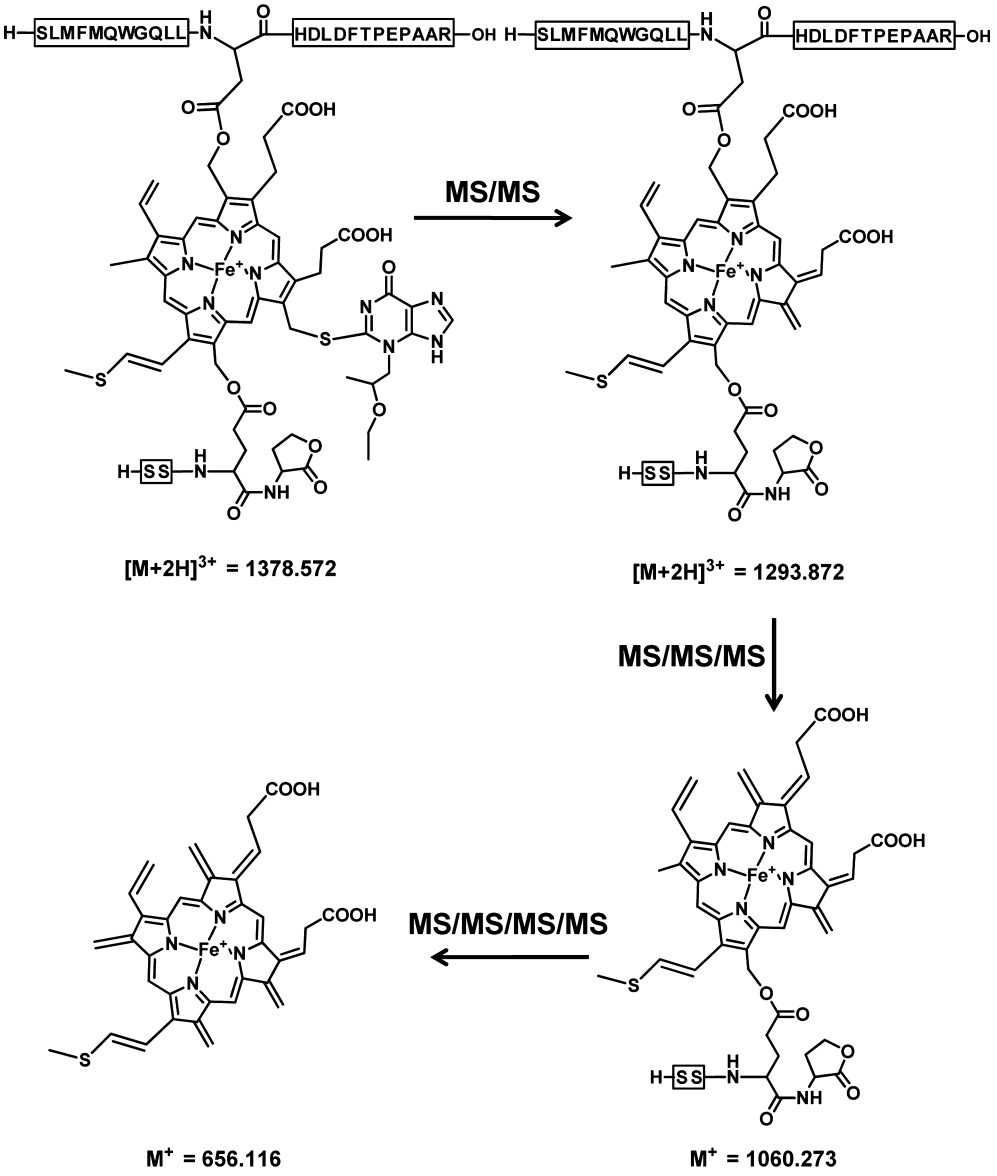

spectrometry allowed stepwise deconstruction of this product in the gas phase. Modification of either peptide moiety was excluded, leaving the protoporphyrin IX ring system of heme as the only eligible site, and the conclusion was reinforced by the respective masses of the heme residues from unmodified and modified MPO. While MPO-catalyzed oxidative coupling of the 254 Da thioxanthine **1** to heme added 252 Da to the protein, CID expelled 254 Da from the molecule. The resulting 2 Da mass deficit was located in the heme group of modified MPO, confirming it as the site of attachment.

CID of heme (M^+, $C_{34}H_{32}N_4O_4$) characteristically results in sequential neutral loss of two carboxymethyl radical species,[38,39] but no such loss was observed during three steps of CID conducted on $[M + 2H]^{3+}$ for the **1**-modified peptide–heme–peptide fragment (Figure 5) and daughter ions that descended from it. [We confirmed the same behavior of horse myoglobin-derived heme through MS^3 using the LTQ spectrometer (data not shown).] Progressively increasingly energetic CID has been used to estimate relative bond strengths in the native heme system, with the dissociation bond energy for the first carboxymethyl group estimated to be 2.4 eV[39] (55 kcal/mol). As the thioether bond from heme to **1** and both ester bonds from heme to carboxylate side chains all broke more readily than the bonds to the carboxymethyl group, the bonds ligating heme to extraneous groups are clearly weaker than the bonds connecting its ring to its own substituents.

The exact locus of modification of heme in MPO by **1** was not defined by mass spectrometry, but reference to the X-ray structure of MPO[40] suggested that the relatively exposed substituents of the heme pyrrole D-ring or the nearby *meso* carbons were the most feasible sites for modification. Defining this exactly required a direct structural study by X-ray crystallography, which showed that the methyl substituent of the heme D-ring was the site of reaction. Despite the steric factors that appeared to favor this outcome, it was only one among several reasonable possibilities.

For example, heme vinyl groups are the target of activity-based halogenations of heme in horseradish peroxidase (HRP).

dx.doi.org/10.1021/bi201872j | *Biochemistry* 2012, 51, 2065–2077

Table 1. Data Collection and Refinement Statistics

	(A) Data Collection
space group	$P2_1$
unit cell dimensions	a = 63.8 Å, b = 242.6 Å, c = 151.5 Å, β = 91.2°
resolution (Å)	152−2.0
completeness (%)[a]	98.5 (96.6)
R_{sym} [a,b]	0.102 (0.531)
$\langle I/\sigma(I)\rangle$[a]	8.2 (2.0)
redundancy[a]	3.4 (3.0)
	(B) Refinement
R_{work} [c]	0.199
R_{free} [c]	0.249
no. of amino acid residues	4560
no. of waters	2503
average B (Å^2)	9.0
rmsd for bond lengths (Å)	0.01
rmsd for bond angles (deg)	1.146
Ramachandran outliers (%)	2.4

[a]Values for the outer resolution shell are given in parentheses. [b]$R_{sym} = \sum_{hkl}(|I_{hkl} - \langle I_{hkl}\rangle|)/\sum_{hkl}\langle I_{hkl}\rangle$, where I_{hkl} is the intensity of reflection hkl and $\langle I_{hkl}\rangle$ is the average intensity of multiple observations. [c]$R_{work} = \sum|F_o - F_c|/\sum F_o$, where F_o and F_c are the observed and calculated structure factor amplitudes, respectively. R_{free} is the R factor for a randomly selected 5% of reflections that were not used in the refinement.

Huang et al.[41] took advantage of the absence of the heme−polypeptide covalent linkage in HRP to reconstitute the enzyme with strategically altered heme analogues that allowed the reaction sites to be specified. A recognized oxidative pathway to one of two alternative products was proposed, with HOBr generated by reaction of bromide with HRP compound I and then addition to the vinyl group to give a bromohydrin. This was the only outcome detected at the 2-vinyl group. At the 4-vinyl substituent group, formation of a vinyl bromide occurred as an alternative outcome. This was proposed to be due to the absence of water molecules near the 4-vinyl group, possibly permitting a nearby group in the polypeptide chain to serve as a general base and steer the reaction to the vinyl bromide rather than the bromohydrin.

In MPO, the 2-vinyl group is already cross-linked to Met409 by a mechanism that requires no enzymatic activity other than that of MPO itself.[16] As an example of related studies, soybean ascorbate peroxidase has been shown to form a cross-link between Trp41 and a heme vinyl group in the presence of hydrogen peroxide[33] with radical chemistry proposed for the mechanism. The generalized view of this and related processes is that proper spatial positioning of protein groups relative to heme, together with the innate capacity of heme for catalytic redox cycling, is all that is needed to engender heme−protein cross-links.[3,42] The main suggestions concerning the function of these cross-links are that they help to protect the enzyme against self-inactivation[43] and fine-tune its catalytic potential[44] by controlling the position and planarity of the heme.

The general nature of the MPO activity-based chemistry that occurs with **1** must be similar to that described for halogenation of HRP. Entry of **1** into the enzyme active site must create a reactive derivative that couples to heme, with the net loss of 2 Da from heme and **1** that accompanies the condensation supporting an oxidative or radical mechanism. If **1** is considered as its thioenol tautomer, activation of the thiol function to a sulfenic acid could reasonably be the starting point, and the rationale given in 1988 by Doerge[32] for peroxide-dependent

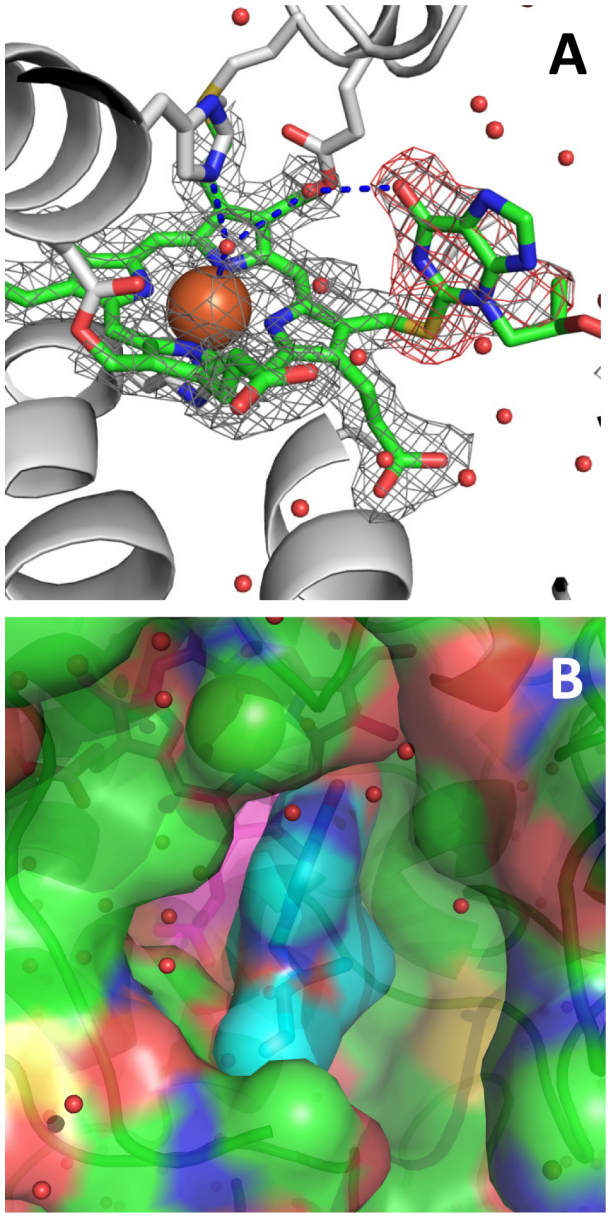

Figure 6. (A) Structure of the MPO active site (dimer A/C) with heme and the heme-linked thioxanthine **1** colored as follows: green for C, red for O, blue for N, and yellow for S. Thioxanthine **1** is shown covalently attached at the methyl group of the heme D-ring. The electron density maps are SigmaA-weighted $2F_o - F_c$ (gray) or $F_o - F_c$ (red) maps, computed prior to the incorporation of thioxanthine **1** into the structure, and clearly show the position and orientation of the thioxanthine moiety. Crystallographic waters are shown as small red spheres, and hydrogen bonds among the waters, protein, and compound are depicted as blue dashed lines. (B) Surface rendering of the crystal structure showing that covalent addition of thioxanthine **1** to heme sterically blocks the MPO active site. The entrance to the MPO active site is shown as a transparent surface, with the carbon atoms of heme colored magenta and other atoms colored as follows: green for C, red for O, blue for N, and yellow for S. Bonds between the atoms of heme and thioxanthine **1** are shown as sticks, with the central Fe seen through the MPO surface as a large sphere. Crystallographic water molecules are depicted as small red spheres, and thioxanthine **1** is depicted as a transparent surface with cyan carbon atoms. Some space remaining to its left is occupied by crystallographic water molecules. This figure was prepared with PyMOL (Schrödinger, LLC).

dx.doi.org/10.1021/bi201872j | *Biochemistry* 2012, 51, 2065−2077

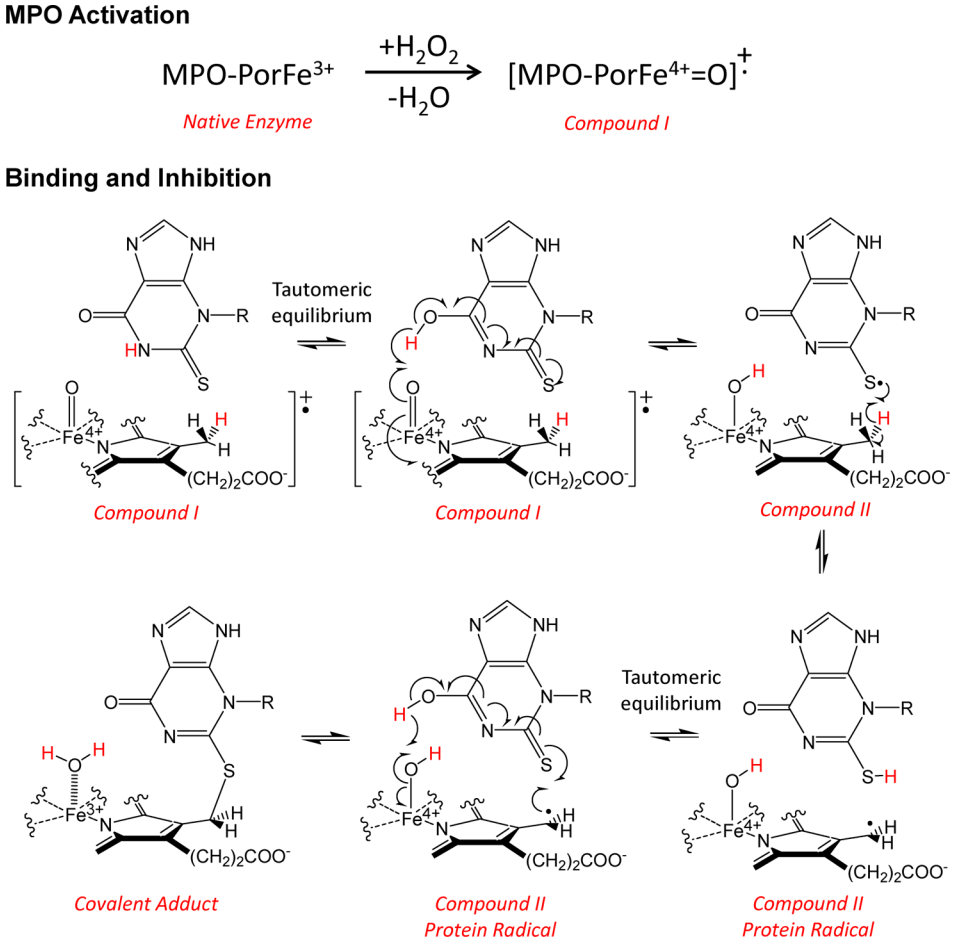

Figure 7. Proposed mechanism for covalent modification of MPO by thioxanthine **1**.

suicide inhibition of lactoperoxidase by 1-methylimidazoline 2-thione would cover the present case well. However, for the following reasons, this does not appear to be the relevant pathway.

Mass spectrometry indicated the formation of a covalent adduct between MPO and **1** with oxidative loss of two hydrogens. The crystal structure specifies the exact location of the adduct and also contributed important information regarding the oxidation state of the iron. It displays an iron−oxygen bond length of 2.7 Å, much longer than the typical values of ∼1.65 and ∼1.82 Å for Fe^{4+}═O and Fe^{4+}−OH bonds, respectively, according to iron K-edge X-ray absorption spectroscopy.[45] The longer bond length suggests the iron in the covalent complex exists in an Fe^{3+} oxidation state and is coordinated to a water molecule, which is also its condition in the resting enzyme. The iron oxidation state for the gas-phase unmodified and **1**-modified peptide−heme−peptide fragments was clearly determined as Fe^{3+} based on accurate mass measurements and isotopic distribution simulations, and it remained the same (Fe^{3+}) for all CID fragment ions containing heme observed in multistage mass spectrometry.

On the basis of the experimental findings, a radical-based mechanism for the inhibition of MPO by **1** can be proposed (Figure 7). This is generally similar to the proposal already published for a similar compound,[14] but an appealing feature of our mechanism is that the binding mode for **1** in its noncovalent complex with MPO resembles its positioning in the crystal structure of the covalent adduct. The mechanism requires very little maneuvering by the inhibitor in the binding site in all of its steps and suggests reasons why thiouracil is such a privileged scaffold for MPO inactivation. In the first step, oxidation of MPO by H_2O_2 generates compound I, which then binds noncovalently to the inhibitor. Because of the proximity of the carbonyl oxygen of **1** to the oxygen atom bound to Fe^{4+}, a tautomeric equilibrium between the NH and OH forms is postulated as the first step after compound binding. Although quantum mechanical calculations in water indicate NH ≫ OH > SH as the order for the tautomeric forms of **1** (see Experimental Procedures), their relative stability might be altered in the protein-bound form. Therefore, the transition from compound I to II occurs upon transfer of a hydrogen atom (or a stepwise single-electron transfer followed by a proton) from the inhibitor OH group leading to the radical species **1**•. It is plausible that the transfer of a hydrogen atom from the D-ring methyl group to the S atom of **1**• restores **1**, as this reaction would provide a more stable radical (compound II protein radical) because of extensive conjugation in the heme. A radical at this position in heme was proposed in studies with horseradish peroxidase that modeled the chemistry required for formation of heme−peptide cross-links in MPO.[46] Another tautomeric equilibrium, now between the SH and OH forms, is then necessary to facilitate the second transfer of a hydrogen atom from **1**, possibly the same molecule as the one used in the first transfer. In this case, hydrogen is transferred to the OH group on iron to generate a water molecule and reduce Fe^{4+} to Fe^{3+}, recreating **1**• and allowing formation of the covalent

dx.doi.org/10.1021/bi201872j | *Biochemistry* 2012, 51, 2065−2077

adduct between **1** and the heme. The proposed mechanism then suggests that the water molecule generated in the final step is composed of the two hydrogens lost upon adduct formation, one from the heme and the other from the inhibitor (see hydrogens colored red in Figure 7).

An alternative to the second tautomerization step would be transfer of the electron from the methylene radical to iron, reducing it to the ferric, water-bound state and leaving a methylene cation that could react directly with the thiol of **1**. We are indebted to an anonymous reviewer for this proposal, which aligns well with earlier accounts of the formation of heme−polypeptide ester bonds in mammalian peroxidases.[16]

The X-ray structure of **1**-modified MPO (Figure 6) shows that the covalently attached residue of **1** largely occludes the channel leading from the exterior to the cavity that contains the heme. This would certainly prevent any organic substrate such as uric acid from reaching the active center, but it is not self-evident that the intrinsic catalytic potential of the active center has been eliminated.

The structure presented here is in excellent agreement with the recently published crystal structures of MPO covalently modified by two other thioxanthines denoted TX2 and TX5.[14] Salient structural features from the earlier work, notably the positioning of the inhibitor relative to the D-ring methyl group, the perpendicular orientation of the thioxanthine relative to the plane of the heme, and the inherent flexibility of the covalently bound ligand leading to a high degree of disorder in the active site, are observed and refined to higher resolution in this work. Direct structural comparison of the MPO−**1** complex (PDB entry 4DL1) with PDB entries 3ZS0 and 3ZS1 (corresponding to the MPO−TX2 and MPO−TX5 structures, respectively) indicates nearly identical overall geometry, with subtle differences most likely attributable to differences in resolution (2.0 Å for the MPO−**1** complex, 2.3 Å for 3ZS0, and 2.6 Å for 3ZS1).

In addition to strengthening our understanding of the structural basis for the inactivating effects of MPO inhibitors related to 3-propyluracil[12] and thioxanthine,[14] the methods and results presented here open a new route to the analysis of complex heme-containing peptides by multistage high-resolution mass spectrometry. The work helps to set the stage for continued and increasingly knowledge-based development of therapeutic agents directed against MPO and other hemoproteins.

■ ASSOCIATED CONTENT

Ⓢ Supporting Information

Figures S1 and S2. This material is available free of charge via the Internet at http://pubs.acs.org.

Accession Codes

A structure has been deposited as Protein Data Bank entry 4DL1.

■ AUTHOR INFORMATION

Corresponding Author

*Phone: (860) 441-3601. E-mail: kieran.f.geoghegan@pfizer.com.

Funding

This work was supported by Pfizer Inc.

Notes

While contributing to this study, all authors were employed by Pfizer Inc., which was the sole source of funding for the work. K.F.G., A.H.V., X.F., A.J.B., R.B.R., K.A., P.A.C., C.R.W.G., and F.F.V. are current employees of Pfizer. S.V.F. is now at Esperion Therapeutics (Plymouth, MI). J.J.C. and S.N.S. both have no relevant business address. S.J.C. is currently a graduate student at Western Michigan University (Kalamazoo, MI).

■ ACKNOWLEDGMENTS

Use of IMCA-CAT beamline 17-ID at the Advanced Photon Source was supported by the companies of the Industrial Macromolecular Crystallography Association through a contract with Hauptman-Woodward Medical Research Institute. Use of the Advanced Photon Source was supported by the U.S. Department of Energy, Office of Science, Office of Basic Energy Sciences, under Contract DE-AC02-06CH11357. We thank T. J. McLellan and L. R. Hoth for assistance.

■ ABBREVIATIONS

MPO, myeloperoxidase; CID, collision-induced dissociation; fwhm, full width at half-maximum (applied to spectral peak width, and therefore to the resolution achieved by a spectrometer); *m*/*z*, mass-to-charge ratio; PDB, Protein Data Bank.

■ REFERENCES

(1) Davies, M. J., Hawkins, C. L., Pattison, D. I., and Rees, M. D. (2008) Mammalian heme peroxidases: From molecular mechanisms to health implications. *Antioxid. Redox Signaling 10*, 1199−1234.

(2) Hansson, M., Olsson, I., and Nauseef, W. M. (2006) Biosynthesis, processing, and sorting of human myeloperoxidase. *Arch. Biochem. Biophys. 445*, 214−224.

(3) Furtmüller, P. G., Zederbauer, M., Jantschko, W., Helm, J., Bogner, M., Jakopitsch, C., and Obinger, C. (2006) Active site structure and catalytic mechanisms of human peroxidases. *Arch. Biochem. Biophys. 445*, 199−213.

(4) Klebanoff, S. J. (2005) Myeloperoxidase: Friend and foe. *J. Leukocyte Biol. 77*, 598−625.

(5) Harrison, J. E., and Schultz, J. (1976) Studies on the chlorinating activity of myeloperoxidase. *J. Biol. Chem. 251*, 1371−1374.

(6) van Dalen, C. J., Whitehouse, M. W., Winterbourn, C. C., and Kettle, A. J. (1997) Thiocyanate and chloride as competing substrates for myeloperoxidase. *Biochem. J. 327*, 487−492.

(7) Meotti, F. C., Jameson, G. N. L., Turner, R., Harwood, D. T., Stockwell, S., Rees, M. D., Thomas, S. R., and Kettle, A. J. (2011) Urate as a physiological substrate for myeloperoxidase. *J. Biol. Chem. 286*, 12901−12911.

(8) Choi, D.-K., Pennathur, S., Perier, C., Tieu, K., Teismann, P., Wu, D.-C., Jackson-Lewis, V., Vila, M., Vonsattel, J.-P., Heinecke, J. W., and Przedborski, S. (2005) Ablation of the inflammatory enzyme myeloperoxidase mitigates features of Parkinson's disease in mice. *J. Neurosci. 25*, 6594−6600.

(9) Wang, Z., Nicholls, S. J., Rodriguez, E. R., Kummu, O., Horkko, S., Barnard, J., Reynolds, W. F., Topol, E. J., DiDonato, J. A., and Hazen, S. L. (2007) Protein carbamylation links inflammation, smoking, uremia and atherogenesis. *Nat. Med. 13*, 1176−1184.

(10) Shao, B.-H., Oda, M. N., Oram, J. F., and Heinecke, J. W. (2010) Myeloperoxidase: An oxidative pathway for generating dysfunctional high-density lipoprotein. *Chem. Res. Toxicol. 23*, 447−454.

(11) Malle, E., Furtmüller, P. G., Sattler, W., and Obinger, C. (2007) Myeloperoxidase: A target for new drug development? *Br. J. Pharmacol. 152*, 838−854.

(12) Lee, E., Miki, Y., Katsljra, H., and Kariya, K. (1990) Mechanism of inactivation of myeloperoxidase by propylthiouracil. *Biochem. Pharmacol. 39*, 1467−1471.

(13) Lee, E., Hirouchi, M., Hosokawa, M., Sayo, H., Kohno, M., and Kariya, K. (1988) Inactivation of peroxidases of rat bone marrow by

repeated administration of propylthiouracil is accompanied by a change in the heme structure. *Biochem. Pharmacol. 37*, 2151−2153.
(14) Tidén, A.-K., Sjögren, T., Svensson, M., Bernlind, A., Senthilmohan, R., Auchère, F., Norman, H., Markgren, P.-O., Gustavsson, S., Schmidt, S., Lundquist, S., Forbes, L. V., Magon, N. J., Paton, L. N., Jameson, G. N. L., Eriksson, H., and Kettle, A. J. (2011) 2-Thioxanthines are mechanism-based inactivators of myeloperoxidase that block oxidative stress during inflammation. *J. Biol. Chem. 286*, 37578−37589.
(15) Ortiz de Montellano, P. R. (2008) Mechanism and role of covalent heme binding in the CYP4 family of P450 enzymes and the mammalian peroxidases. *Drug Metab. Rev. 40*, 405−426.
(16) Colas, C., and Ortiz de Montellano, P. R. (2003) Autocatalytic radical reactions in physiological prosthetic heme modification. *Chem. Rev. 103*, 2305−2332.
(17) Arvadia, P., Narwaley, M., Whittal, R. M., and Siraki, A. G. (2011) 4-Aminobenzoic acid hydrazide inhibition of microperoxidase-11: Catalytic inhibition by reactive metabolites. *Arch. Biochem. Biophys. 515*, 120−126.
(18) Vonrhein, C., Flensburg, C., Keller, P., Sharff, A., Smart, O., Paciorek, W., Womack, T., and Bricogne, G. (2011) Data processing and analysis with the autoPROC toolbox. *Acta Crystallogr. D67*, 293−302.
(19) Kabsch, W. (2010) Software XDS for image rotation, recognition and crystal symmetry assignment. *Acta Crystallogr. D66*, 125−132.
(20) Bailey, S. (1994) The CCP4 suite: Programs for protein crystallography. *Acta Crystallogr. D50*, 760−763.
(21) DePillis, G. D., Ozaki, S.-i., Kuo, J. M., Maltby, D. A., and Ortiz de Montellano, P. R. (1997) Autocatalytic processing of heme by lactoperoxidase produces the native protein-bound prosthetic group. *J. Biol. Chem. 272*, 8857−8860.
(22) Taylor, K. L., Strobel, F., Yue, K. T., Ram, P., Pohl, J., Woods, A. S., and Kinkade, J. M. (1995) Isolation and identification of a protoheme IX derivative released during autolytic cleavage of human myeloperoxidase. *Arch. Biochem. Biophys. 316*, 635−642.
(23) Taylor, K. L., Pohl, J., and Kinkade, J. M. Jr. (1992) Unique autolytic cleavage of human myeloperoxidase. Implications for the involvement of active site Met409. *J. Biol. Chem. 267*, 25282−25288.
(24) Olsen, J. V., Schwartz, J. C., Griep-Raming, J., Nielsen, M. L., Damoc, E., Denisov, E., Lange, O., Remes, P., Taylor, D., Splendore, M., Wouters, E. R., Senko, M., Makarov, A., Mann, M., and Horning, S. (2009) A dual pressure linear ion trap Orbitrap instrument with very high sequencing speed. *Mol. Cell. Proteomics 8*, 2759−2769.
(25) Volmer, D. A. (2010) Prerequisites for supplying complementary high-resolution mass spectrometry data in RCM publications. *Rapid Commun. Mass Spectrom. 24*, 3499−3500.
(26) Feng, X., and Siegel, M. (2007) FTICR-MS applications for the structure determination of natural products. *Anal. Bioanal. Chem. 389*, 1341−1363.
(27) McCoy, A. J., Grosse-Kunstleve, R. W., Adams, P. D., Winn, M. D., Storoni, L. C., and Read, R. J. (2007) *Phaser* crystallographic software. *J. Appl. Crystallogr. 40*, 658−674.
(28) Fiedler, T. J., Davey, C. A., and Fenna, R. E. (2000) X-ray crystal structure and characterization of halide-binding sites of human myeloperoxidase at 1.8 Å resolution. *J. Biol. Chem. 275*, 11964−11971.
(29) Murshudov, G. N., Vagin, A. A., and Dodson, E. J. (1997) Refinement of macromolecular structures by the maximum-likelihood method. *Acta Crystallogr. D53*, 240−255.
(30) Murzin, A. G., Brenner, S. E., Hubbard, T., and Chothia, C. (1995) SCOP: A structural classification of proteins database for the investigation of sequences and structures. *J. Mol. Biol. 247*, 536−540.
(31) Blair-Johnson, M., Fiedler, T., and Fenna, R. (2001) Human myeloperoxidase: Structure of a cyanide complex and its interaction with bromide and thiocyanate substrates at 1.9 Å resolution. *Biochemistry 40*, 13990−13997.
(32) Doerge, D. R. (1988) Mechanism-based inhibition of lactoperoxidase by thiocarbamide goitrogens. Identification of turnover and inactivation pathways. *Biochemistry 27*, 3697−3700.
(33) Pipirou, Z., Bottrill, A. R., Metcalfe, C. M., Mistry, S. C., Badyal, S. K., Rawlings, B. J., and Raven, E. L. (2007) Autocatalytic formation of a covalent link between tryptophan 41 and the heme in ascorbate peroxidase. *Biochemistry 46*, 2174−2180.
(34) Siraki, A. G., Deterding, L. J., Bonini, M. G., Jiang, J., Ehrenshaft, M., Tomer, K. B., and Mason, R. P. (2008) Procainamide, but not N-acetylprocainamide, induces protein free radical formation on myeloperoxidase: A potential mechanism of agranulocytosis. *Chem. Res. Toxicol. 21*, 1143−1153.
(35) Bandyopadhyay, U., Bhattacharyya, D. K., and Banerjee, R. K. (1993) Mechanism-based inactivation of gastric peroxidase by mercaptomethylimidazole. *Biochem. J. 296*, 79−84.
(36) Doerge, D. R. (1986) Mechanism-based inhibition of lactoperoxidase by thiocarbamide goitrogens. *Biochemistry 25*, 4724−4728.
(37) Wojciechowski, G., Huang, L., and Ortiz de Montellano, P. R. (2005) Autocatalytic modification of the prosthetic heme of horseradish but not lactoperoxidase by thiocyanate oxidation products. A role for heme-protein covalent cross-linking. *J. Am. Chem. Soc. 127*, 15871−15879.
(38) Chiavarino, B., Crestoni, M. E., Fornarini, S., and Rovira, C. (2007) Protonated heme. *Chem.— Eur. J. 13*, 776−785.
(39) Charkin, O. P., Klimenko, N. M., Nguyen, P. T., Charkin, D. O., Mebel, A. M., Lin, S. H., Wang, Y. S., Wei, S. C., and Chang, H. C. (2005) Fragmentation of heme and hemin$^+$ with sequential loss of carboxymethyl groups: A DFT and mass-spectrometry study. *Chem. Phys. Lett. 415*, 362−369.
(40) Fenna, R., Zeng, J., and Davey, C. (1995) Structure of the green heme in myeloperoxidase. *Arch. Biochem. Biophys. 316*, 653−656.
(41) Huang, L., Wojciechowski, G., and Ortiz de Montellano, P. R. (2005) Prosthetic heme modification during halide ion oxidation. Demonstration of chloride oxidation by horseradish peroxidase. *J. Am. Chem. Soc. 127*, 5345−5353.
(42) Pipirou, Z., Bottrill, A. R., Svistunenko, D. A., Efimov, I., Basran, J., Mistry, S. C., Cooper, C. E., and Raven, E. L. (2007) The reactivity of heme in biological systems: Autocatalytic formation of both tyrosine−heme and tryptophan−heme covalent links in a single protein architecture. *Biochemistry 46*, 13269−13278.
(43) Huang, L., Wojciechowski, G., and Ortiz de Montellano, P. R. (2006) Role of heme-protein covalent bonds in mammalian peroxidases: Protection of the heme by a single engineered heme-protein link in horseradish peroxidase. *J. Biol. Chem. 281*, 18983−18988.
(44) Brogioni, S., Stampler, J., Furtmüller, P. G., Feis, A., Obinger, C., and Smulevich, G. (2008) The role of the sulfonium linkage in the stabilization of the ferrous form of myeloperoxidase: A comparison with lactoperoxidase. *Biochim. Biophys. Acta 1784*, 843−849.
(45) Newcomb, M., Halgrimson, J. A., Horner, J. H., Wasinger, E. C., Chen, L. X., and Sligar, S. G. (2008) X-ray absorption spectroscopic characterization of a cytochrome P450 compound II derivative. *Proc. Natl. Acad. Sci. U.S.A. 105*, 8179−8184.
(46) Colas, C., and de Montellano, P. R. O. (2004) Horseradish peroxidase mutants that autocatalytically modify their prosthetic heme group. *J. Biol. Chem. 279*, 24131−24140.